Supporting Information

Mesh-like $LiZnBO_3$/C composites as a prominent stable anode for lithium ion rechargeable batteries

Aihua Li, Liqiang Xu*, Changming Li* and Yitai Qian

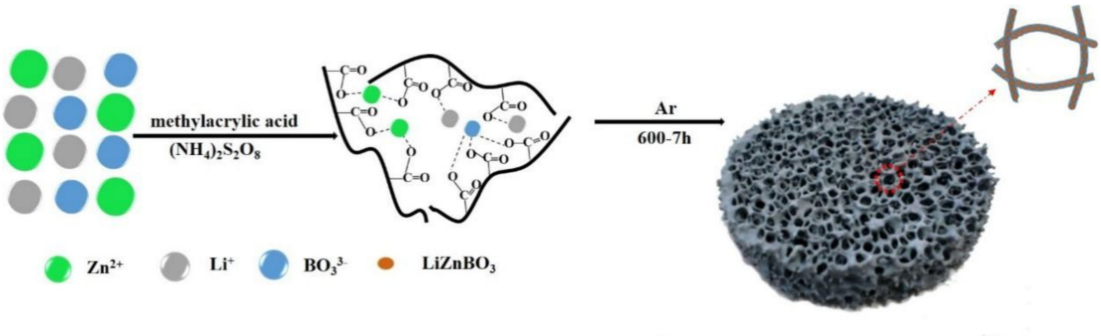

Scheme S1. The formation schematic illustration of the mesh-like $LiZnBO_3$/C.

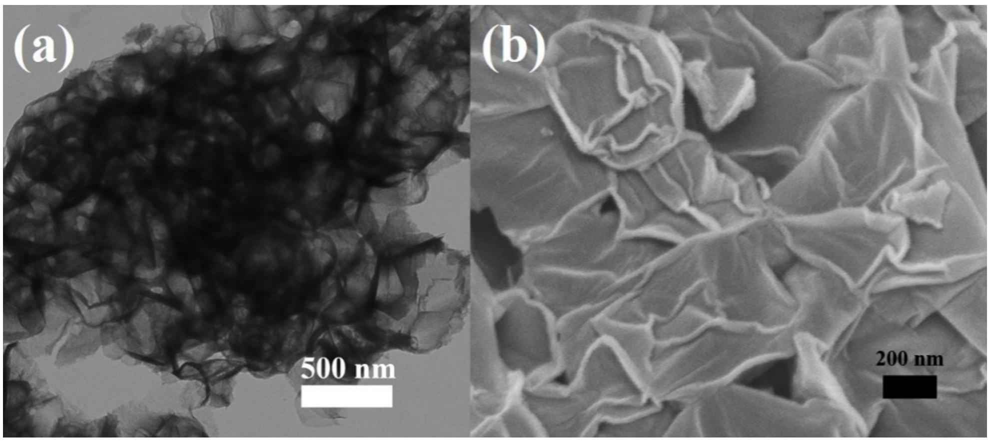

Fig. S1. (a)TEM and (b) FESEM images of the 2D carbon without addition of Li, Zn and B related reagents.

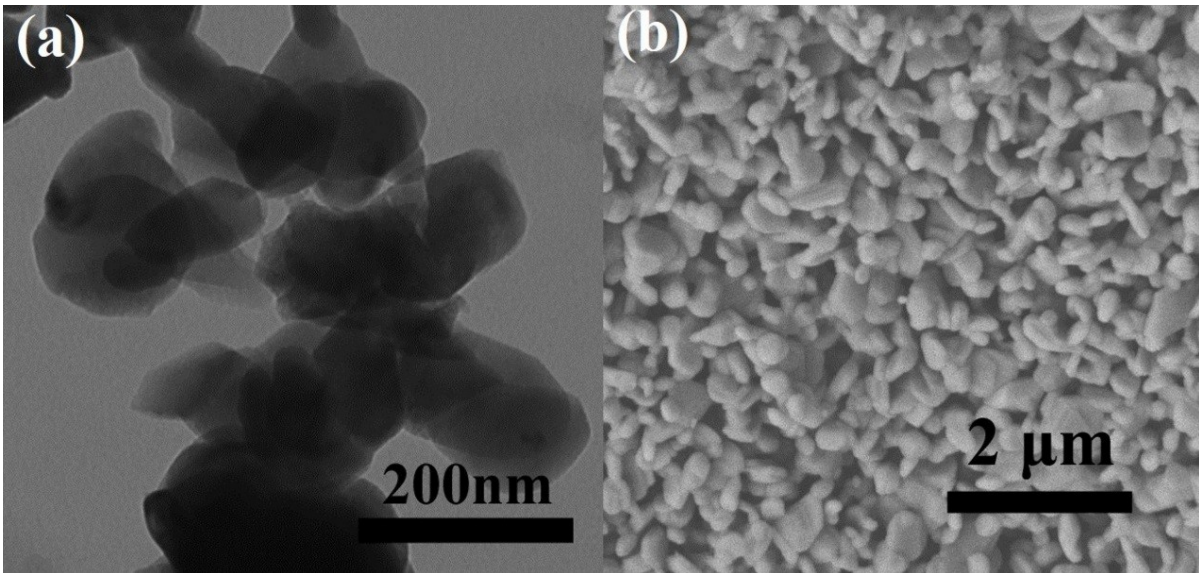

Fig. S2. (a) TEM and (b) FESEM images of the “600-7h Air”.

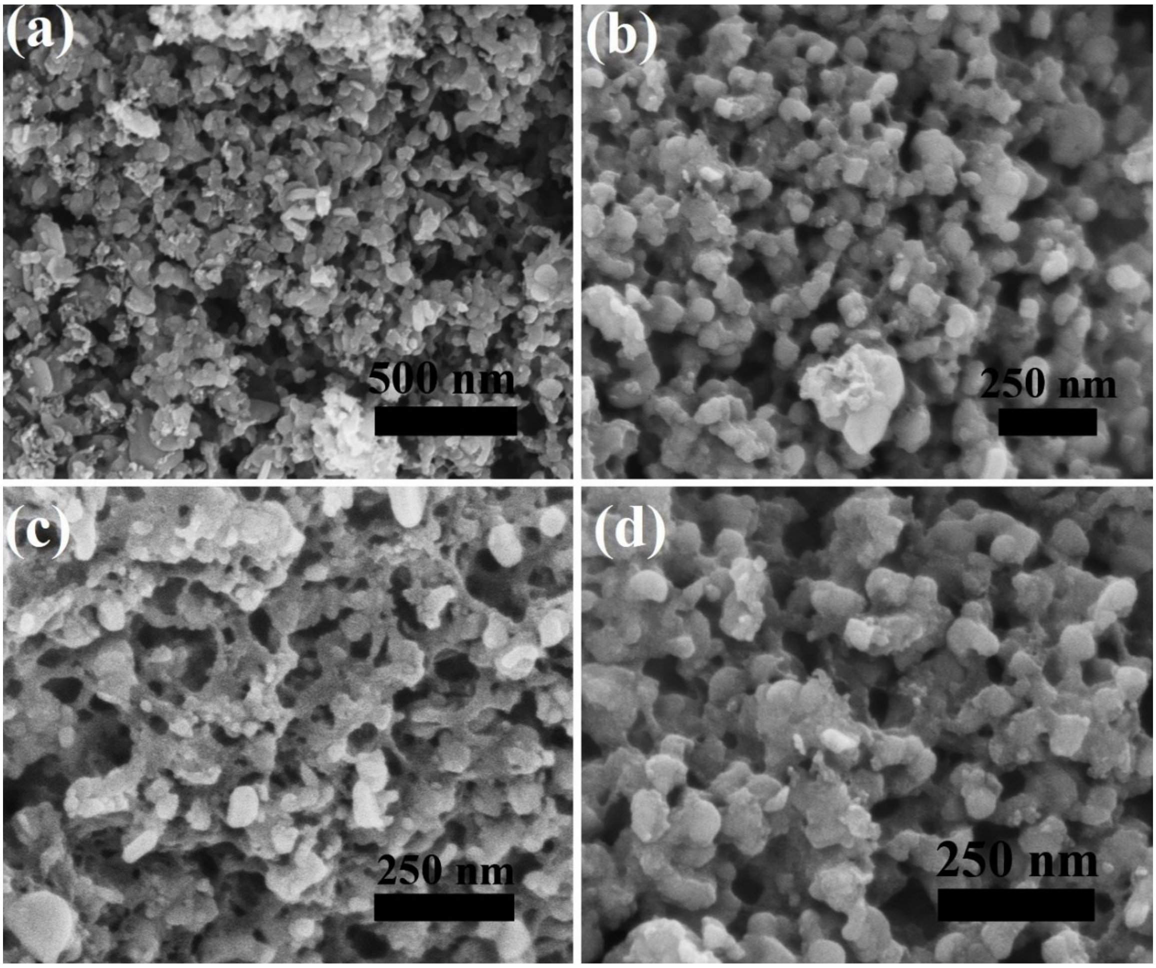

Fig. S3. (a-d) FESEM images of the sample calcined at 600℃ in Ar for 2 hours.

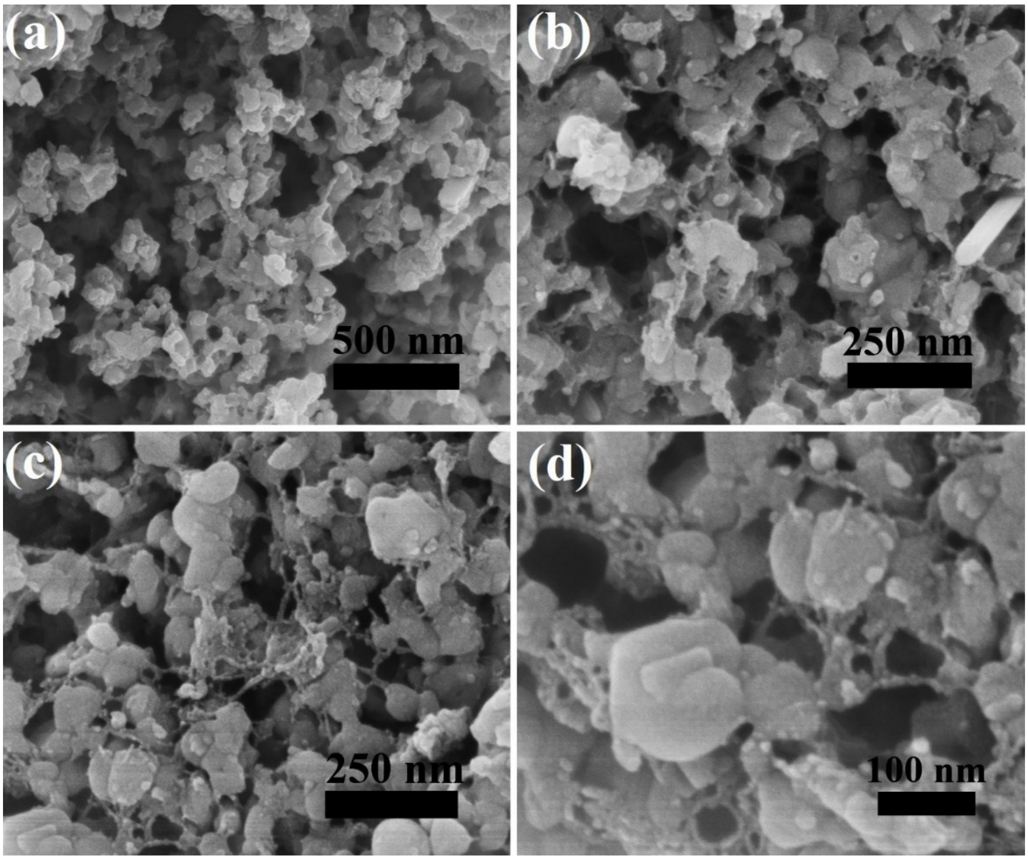

Fig. S4. (a-d) FESEM images of the sample calcined at 600℃ in Ar for 4 hours.

It is note that the raw resources and sebsequent calcination conditions (including calcination time, atmosphere, etc.) are two main factors that affect the morphology of the $LiZnBO_3$/C product. On the one hand, the formation of the mesh-like $LiZnBO_3$/C composite is resulted from the interaction between the Li, Zn, B, C sources (only 2D layered carbon or $LiZnBO_3$ particles could be obtained in the absence of Li, Zn, B or C sources, see Fig. S1 or S2); On the other hand, the size of the $LiZnBO_3$ particles gradually decreased from ~100 nm to 1~2 nm and the mesh-like $LiZnBO_3$/C structure gradually formed upon the calcination time increased from 2 hours to 7 hours (Fig. S3 and S4). When $Zn(NO_3)_2$, $ZnSO_4$, $Zn(OH)_2$ and $ZnCl_2$ were used as different zinc resources, no pure $LiZnBO_3$/C could be obtained except using $Zn(NO_3)_2$ (Fig. S5)

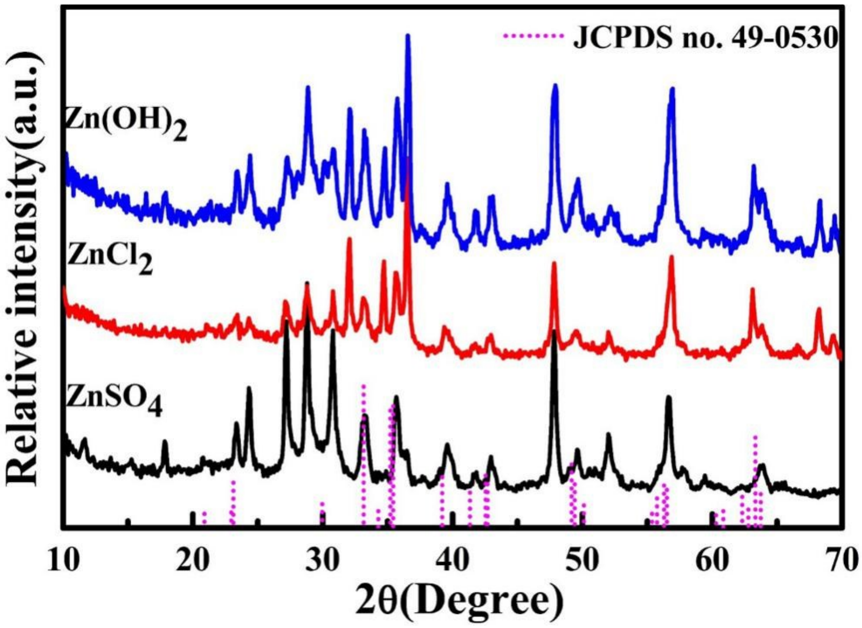

Figure S5. XRD patterns of the samples using $ZnSO_4$, $Zn(OH)_2$ and $ZnCl_2$ as zinc sources.

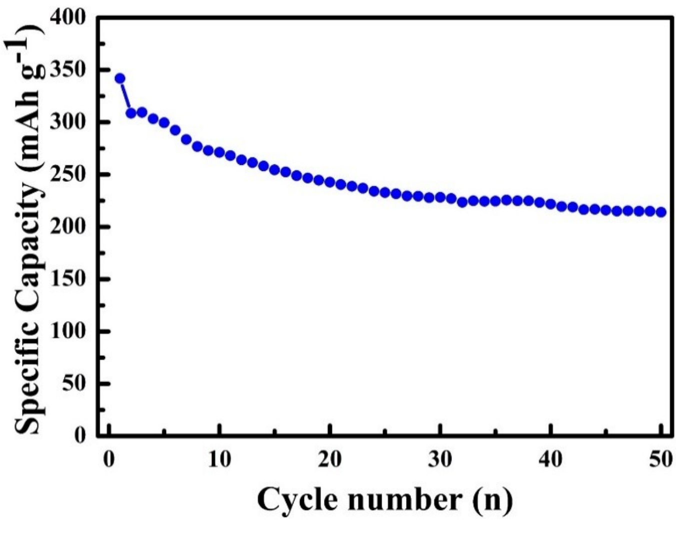

Figure S6. Cycle performance of the 2D carbon at a current density of 100 mA g^{-1}. The initial specific capacity of the pure carbon is 341.9 mAh g^{-1}, which fades to 214.8 mAh g^{-1} after 50 cycles.

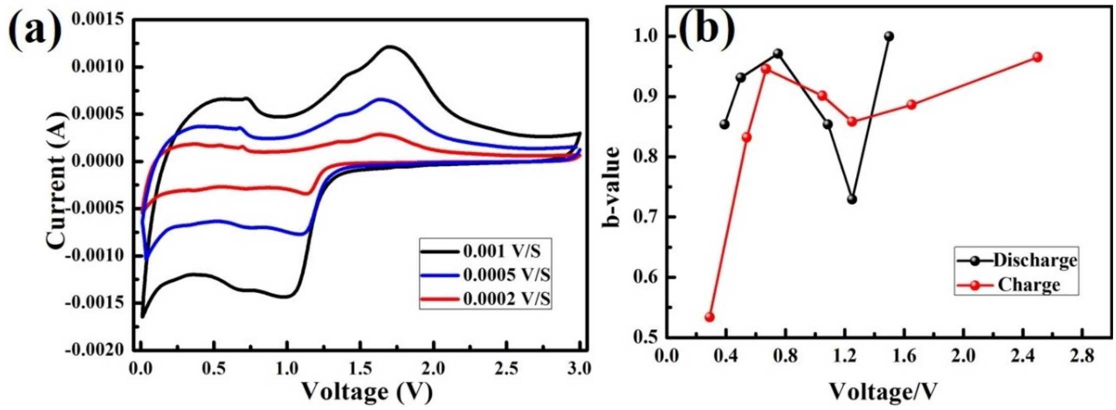

Fig. S7. (a) CV curves of the mesh-like $LiZnBO_3$/C and (b) the corresponding b values vs voltage.

Fig. S7a shows the CV curves of the $LiZnBO_3$/C after 250 cycles under different scanning rates from 0.0002 to 0.001 V/s. The current i obeys a power law relationship with the scanning rate $\boldsymbol{v}$.[1-3] The equation is listed as follows:

$$i = a\,v^b$$

Where b can be used as an important parameter to explain the electrode kinetics. When the b is 0.5, the electrode is controlled by diffusion process originated from the lithium insertion or extraction, while a surface-controlled electrochemical reaction is dominant if the b is 1.0. The calculated b during discharge and charge processes of the $LiZnBO_3$/C is shown in Fig. S7b. During the discharging process, the b is in the range of 0.7 to 1.0, which means that there is a mixed contribution of diffusion and surface-controlled response. The capacity increase after 250 cycles may be resulted from the surface-controlled fast electrochemical reaction, which becomes more and more dominant with the increase of the cycle number. This phenomenon is also reported in previous work.[4]

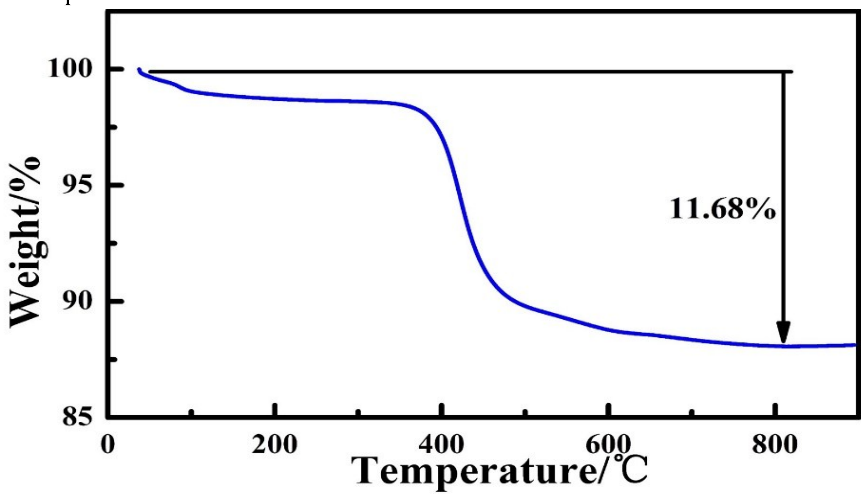

Fig. S8. Thermogravimetric curve of the "600-2h".

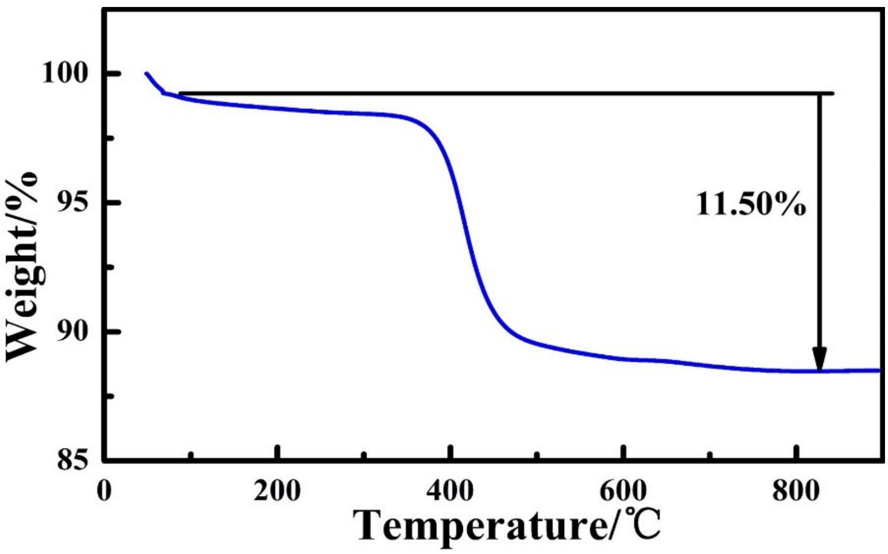

Fig. S9. Thermogravimetric curve of the "600-4h".

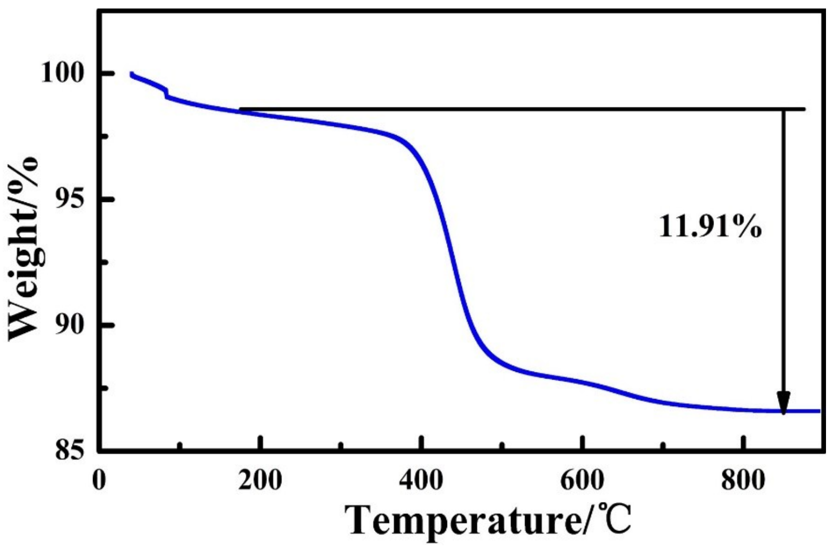

Fig. S10. Thermogravimetric curve of the "600-7h".

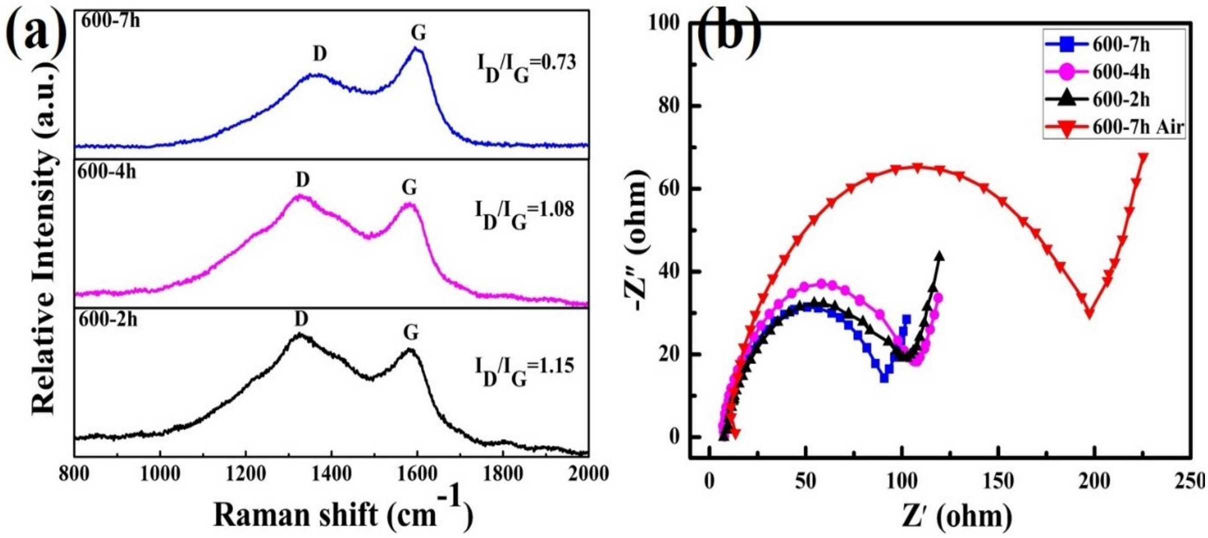

Fig. S11. (a) Raman spectra and (b) EIS spectra of the samples.

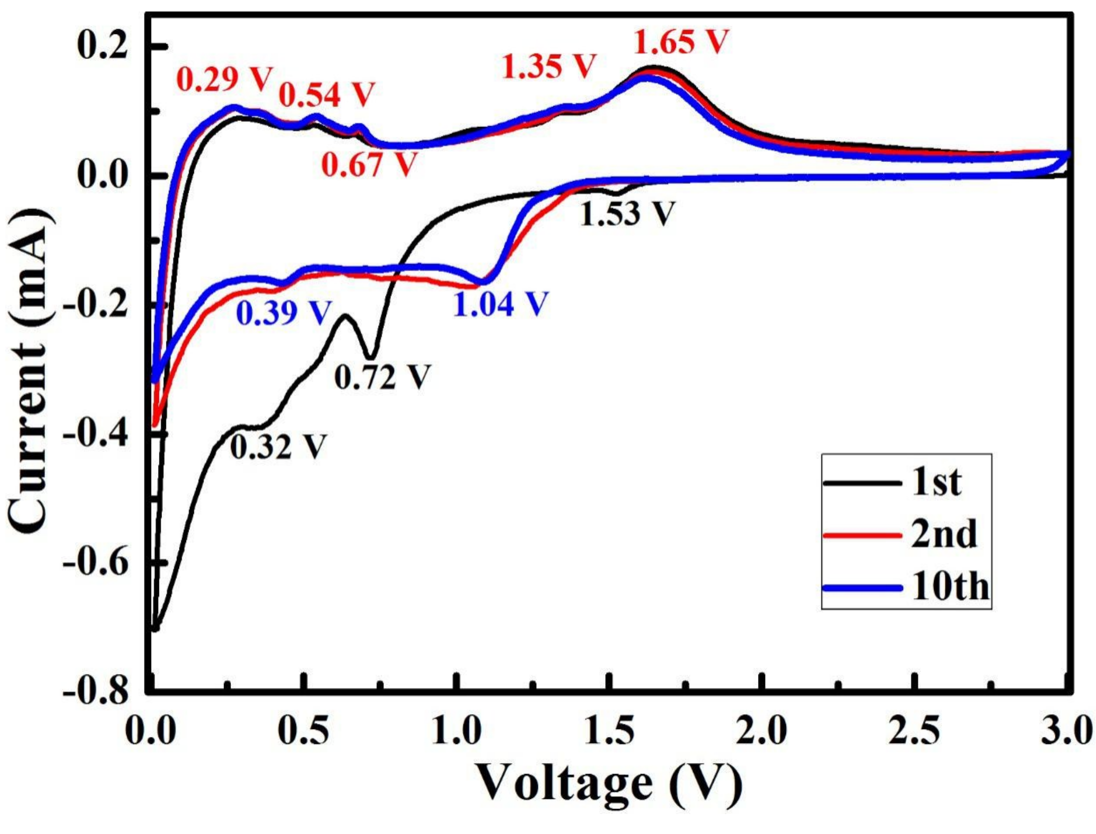

Fig. S12. CV curves of mesh-like $LiZnBO_3$ at a scan rate of 0.1 mV/s in the range of 0.01-3.0 V.

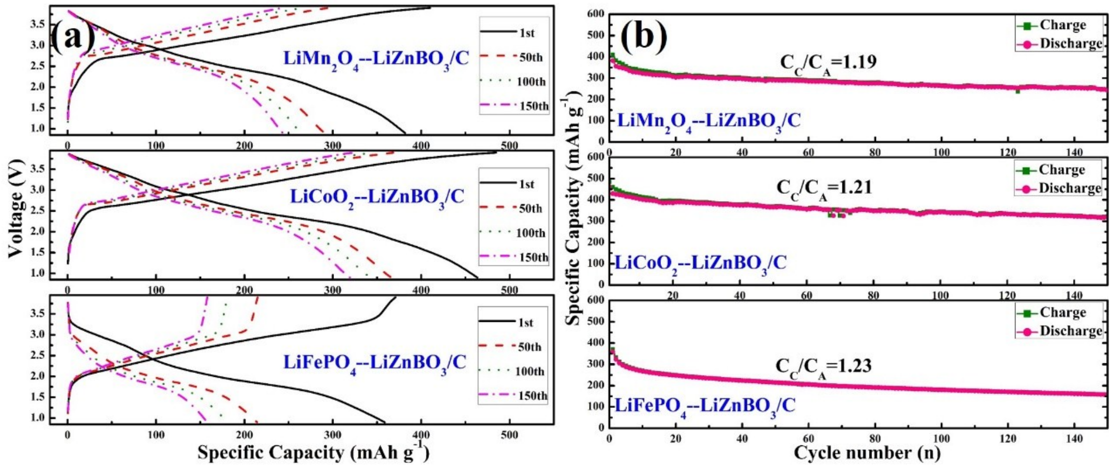

Fig. S13. Electrochemical performances of three different full batteries (a) charging-discharging curves and (b) cycle performances.

The discharge/charge curves of the three full cells are displayed in Fig. S13a. The voltage platforms at around 2.7 V, 2.8 V and 2.2 V are consistent with the plateaus of 1.2 V ($LiZnBO_3/C$) and 3.9 V ($LiCoO_2$), 4.0V ($LiMn_2O_4$) and 3.4V ($LiFePO_4$), respectively. Among the three full cell systems at the similar capacity ratio (C_C/C_A is around 1.2), the $LiCoO_2$-$LiZnBO_3/C$ system exhibited the best cycle performance (Fig. S13b).

In Li-ion batteries, the capacities between cathode and anode materials are different. It is essential to experimentally determine an optimal material ratio of cathode (C_C) to anode (C_A) for good operation. The definitions of C_C and C_A can be

$$C_C(mAh) = C_{practical\ capacity\ of\ cathode}\left(mAh\ g^{-1}\right) \times m_{cathode}\,(g)$$

$$C_A(mAh) = C_{practical\ capacity\ of\ anode}\left(mAh\ g^{-1}\right) \times m_{anode}\,(g)$$

For the $LiCoO_2$-$LiZnBO_3/C$ system, the practical capacity of $LiCoO_2/LiZnBO_3/C$ is 130/726 mAh g^{-1} in the first cycle at 100 mA g-1, respectively. We assembled a series of $LiCoO_2$-$LiZnBO_3/C$ with varied C_C/C_A ratios for performance evaluation as in Table S1, sowing that the capacity increases with the increased C_C/C_A ratio from 0.62 to 1.83. However, with further increase of the ratio the capacity of the full cell decreases to a relatively stable value of ~650 mAh g^{-1}. As a result, an optimal C_C/C_A ratio over a range of 1.68 ~1.83 is selected for the $LiCoO_2$-$LiZnBO_3/C$ cells.

Table S1. Charge/discharge capacities of full $LiCoO_2$-$LiZnBO_3/C$ cells with different C_C/C_A ratios in the first cycle.

C_C/C_A	0.62	0.71	0.88	0.93	1.06	1.68	1.83	1.92	1.94	2.45
1st Charge (mAh g^{-1})	460	509	516	563	691	710	728	644	649	657
1st Discharge (mAh g^{-}	430	448	464	469	650	657	687	603	612	629

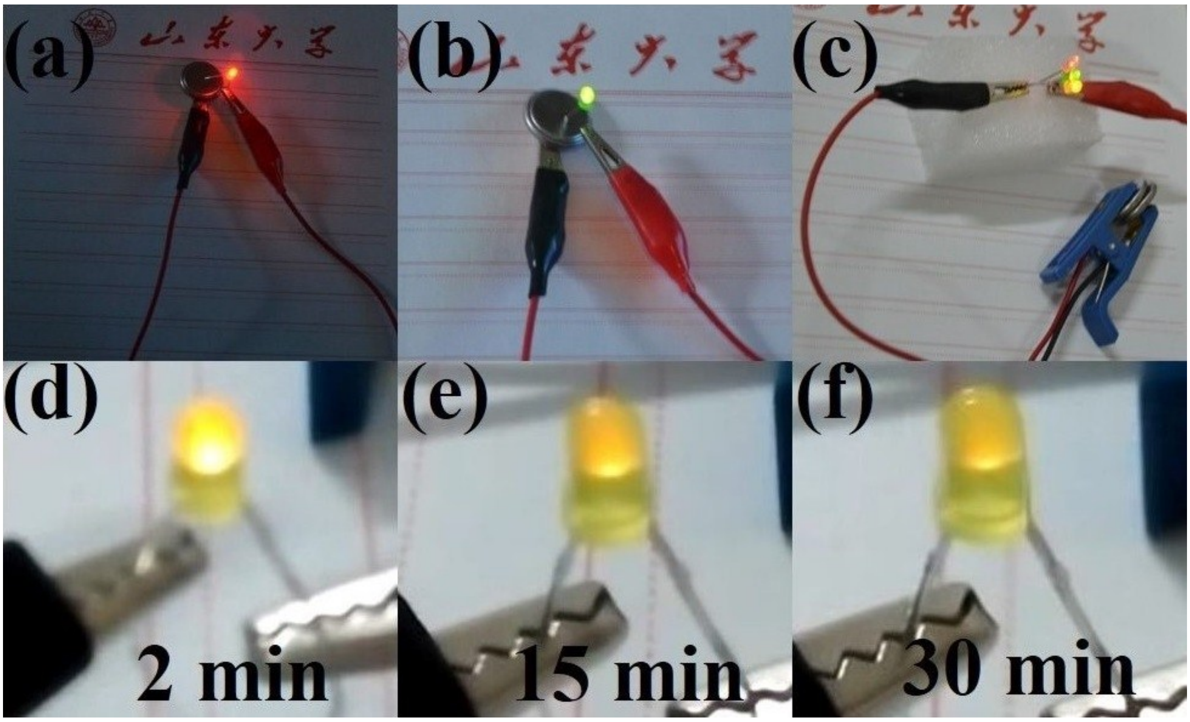

Fig. S14. The performances of the full LIBs after rate performance for 60 cycles: (a,b) an individual full cell could light a red/green LED, (c) two full cells could light three LEDs at the same time and (d-f) keep a yellow LED light for 30 min.

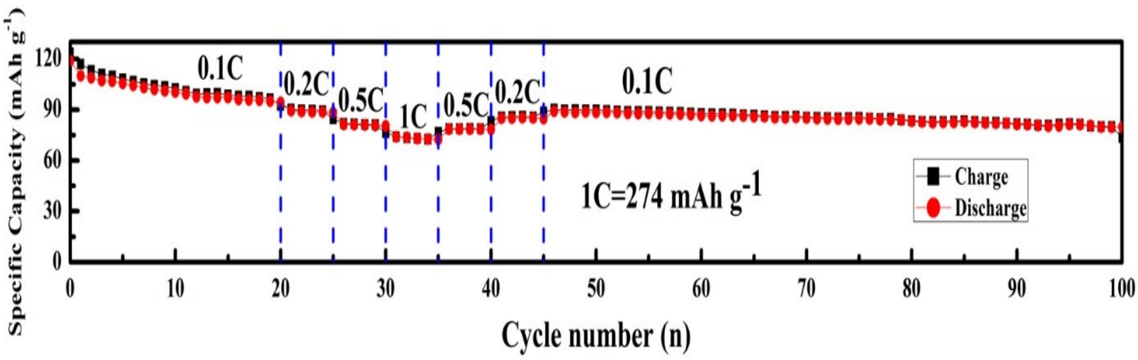

Fig. S15. Rate performance of $LiZnBO_3$/C-$LiCoO_2$ based on the mass of $LiCoO_2$.

References

[1] T. Brezesinski, J. Wang, S.H. Tolbert, B. Dunn, Nat. Mater. 2010, **9**, 146.

[2] V. Augustyn, J. Come, M.A. Lowe, J.W. Kim, P.-L. Taberna, S.H. Tolbert, H.D. Abruna, P. Simon, B. Dunn, Nat. Mater. 2013, **12**, 518.

[3] K. Z. Cao, L. F. Jiao, Y. C. Liu, H. Q. Liu, Y. J. Wang, H. T. Yuan, Adv. Funct. Mater. 2015, **25**, 1082.
[4] Y. L. Zhou, D. Yan, H. Y. Xu, J. K. Feng, X. L. Jiang, J. Yue, J. Yang, Y. T. Qian, Nano Energy 2015, **12**, 528.